Mathematical Geology, Vol. 35, No. 1, January 2003 (© 2003)

Complementary Entropy and Wavelet Analysis of Drilling-Ability Data[1]

G. Frantziskonis[2] and A. Denis[3]

The paper combines wavelet and entropy analysis of nonstationary drilling-ability data in order to obtain optimum information on the mechanical behavior of different geological formations. Both methods are multiscale in nature, and while entropy analysis provides information on stationary subdomains, wavelet analysis identifies dominant scales or range of scales at which the entropy analysis is most useful. The combination of the techniques yields relatively simple results that can aid the drilling process by providing information on delays to be expected.

KEY WORDS: multiscale, nonstationary, spatial series, tunnelling.

INTRODUCTION

Geostatistical analysis based on random field theory of stationary signals has found many applications, to the point that it is regarded by many as the "standard" one. However, it is difficult to apply such analysis to geologic formations of which nonstationarity is an inherent property. Thus, research on the development of tools for the analysis of geological signals, such as those resulting from boring data, is presently very active. It is not intended herein to provide a review of this field; yet, direct reference is given to those works directly relevant to the present study.

Tunnel boring machines record several parameters and thus provide a spatial series of data recorded over a drilling depth of often several hundreds of meters. A combined parameter, i.e., drilling resistance, is directly affected by the properties of the geologic formation, thus detailed knowledge of its variation with depth is

[1]Received 27 October 2001; accepted 19 September 2002.

[2]Department of Civil Engineering and Engineering Mechanics, University of Arizona, Tucson, Arizona 85721; e-mail: frantzis@email.arizona.edu

[3]Centre de Développement des Géosciences Appliquées, Université Bordeaux I, 33405 Talence, France; e-mail: adenis@cdga.u-bordeaux.fr

important for the drilling process. However, drilling resistance spatial series appear to be nonstationary, and this makes their characterization difficult. A method that identifies stationary subregions of the series is desirable, since these regions can then be characterized using "standard" analysis tools. Along these lines, entropy tools are promising, and first attempts in this direction have appeared recently in the literature (Denis and Cremoux, 1999, 2002a; Denis, Cremoux, and Lapeyre, 1998). These tools are multiscale in nature, and can provide information at all scales ranging from the sample support scale (discretization) to the domain scale. Identification of dominant scales or range of scales is thus desirable since that would provide data concentrated on what is useful for the drilling process. This is the central theme of the paper, i.e., using wavelet analysis as a complementary tool capable of identifying dominant scales. Experience along these lines relevant to material problems (Frantziskonis *et al.*, 2000; Frantziskonis and Deymier, 2000; Frantziskonis and Hansen, 2000) proved important for the problems studied herein.

Wavelet analysis is also multiscale, and can be used effectively for the analysis of nonstationary spatial (or time) series. However, the combination of entropy and wavelet analysis can provide relatively simple information on the behavior of different geological formations, which can be used effectively during a tunneling process. None of the two techniques can yield such simple information when used individually.

The remainder of the paper contains the following. A brief introduction to wavelet analysis is followed by the analysis of sample signals and then of actual drilling-ability data. The entropy analysis tool is then presented, and is followed by a section that identifies its relation to wavelet analysis. The complementarily of the two techniques is addressed and how it can be used to yield simple data on the geologic formations is emphasized throughout the paper.

INTRODUCTION TO WAVELET ANALYSIS

Wavelet analysis describes graphs (signals) as superposition of elementary functions. The corresponding description is then used for different purposes, i.e., data compression, feature extraction, pattern recognition, etc. There are several publications on this rather new subject and applications can be found in a wide variety of scientific/engineering fields. Over the past few years, dozens of monographs have appeared in the literature. In one-dimension (extendable to higher ones) a wavelet $\psi(x)$ transforms a fluctuating function $f(x)$ (Daubechies, 1992) according to

$$W_f(a, b) = \int_{-\infty}^{\infty} f(x)\psi_{a,b}(x)\, dx \tag{1}$$

The two-parameter family of functions, $\psi_{a,b}(x) = (1/\sqrt{a})\psi(\frac{x-b}{a})$ is obtained from a single one, ψ, called the mother wavelet, through dilatations by the scaling factor a and translations by the factor b. The factor $1/\sqrt{a}$ is included for normalization purposes. The parameter a can take any positive real value, and the fluctuations of $f(x)$ at position b are measured at the scale a. A wavelet analysis can either be continuous or discrete. The second one, based on an orthogonal decomposition of a signal can be performed with fast algorithms.

Given the wavelet coefficients $W_f(a, b)$ associated with a function f, it is possible to reconstruct f at a range of scales between s_1 and s_2 $(s_1 \leq s_2)$ through the inversion formula

$$f_{s_1,s_2}(x) = \frac{1}{c_\psi} \int_{s_1}^{s_2} \int_{-\infty}^{\infty} W_f(a, b)\psi_{a,b}(x)\, db \frac{da}{a^2} \tag{2}$$

and setting $s_1 \to 0$ and $s_2 \to \infty$.

Wavelet functions used as analyzing wavelets must have zero mean, and in most applications it is imperative that they are orthogonal to some lower order polynomials, i.e.

$$\int x^m \psi(x)\, dx = 0, \quad 0 \leq m \leq n \tag{3}$$

and the maximum vanishing moment, integer n, is directly related to the so-called order of the wavelet. The vanishing moments are important, especially for problems with a "trend" as will be addressed later. In the numerical results presented in this paper, the so-called biorthogonal spline wavelets (Daubechies, 1992) with four vanishing moments were used.

Wavelet Analysis of Example Signals

The first example involves a signal sampled at 1024 discrete and equally spaced points (Fig. 1(a)). It consists of two parts, 512 points each. Both parts are random and stationary, with the same mean and variance; the second part is pure white noise (pure nugget effect) while the first part is spatially correlated as shown in Figure 1(b), with a correlation distance of about 5 spaces. There are 10 scales available, since $2^{10} = 1024$.

Figure 2 shows the plot of the wavelet coefficients obtained from the signal of Figure 1 as well as the energy of the wavelet coefficients as a function of scale, the latter being the dot product of the coefficients with itself. The following are applicable here: the energy of the wavelet coefficients is concentrated towards the fine scales (9 and 10). Part two of the signal (white noise) depicts higher magnitude wavelet coefficients at scale 10 than the first, correlated part. However,

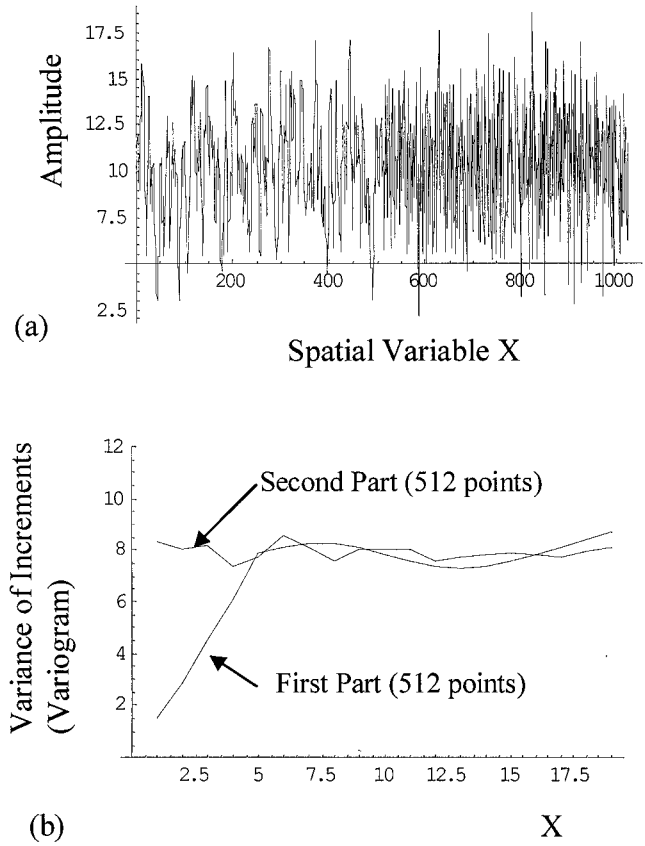

Figure 1. (a) Signal over a space of 1024 points consisting of two parts, 512 points each. (b) The variogram of each of the two parts of (a).

part one shows higher values of the wavelet coefficient at scale 9. Since part two is white noise, naturally the wavelet coefficients increase continuously with finer scales, and their magnitude becomes maximum at the finest scale, i.e., scale 10. Yet, the correlated part of the signal shows maximum value of the wavelet coefficients at scale 9; considering that the correlation distance of part one is approximately 5 space units, and that scale 9 corresponds to 4 spaces (and scale 8 to 8 spaces), it is natural that the wavelet coefficients for this part are of high magnitude at scale 9. As is evident from Figure 2(c), the entire signal has most of its energy at scales 9 and 10. The high value of the energy at scale 10 indicates the presence of white noise (nugget effect) and that at scale 9 shows correlations at that scale (or between scales 9 and 8). In short, study of Figures 2(a–c) provide a clear picture of the nature of the signal, which is overall nonstationary but piece-wise stationary.

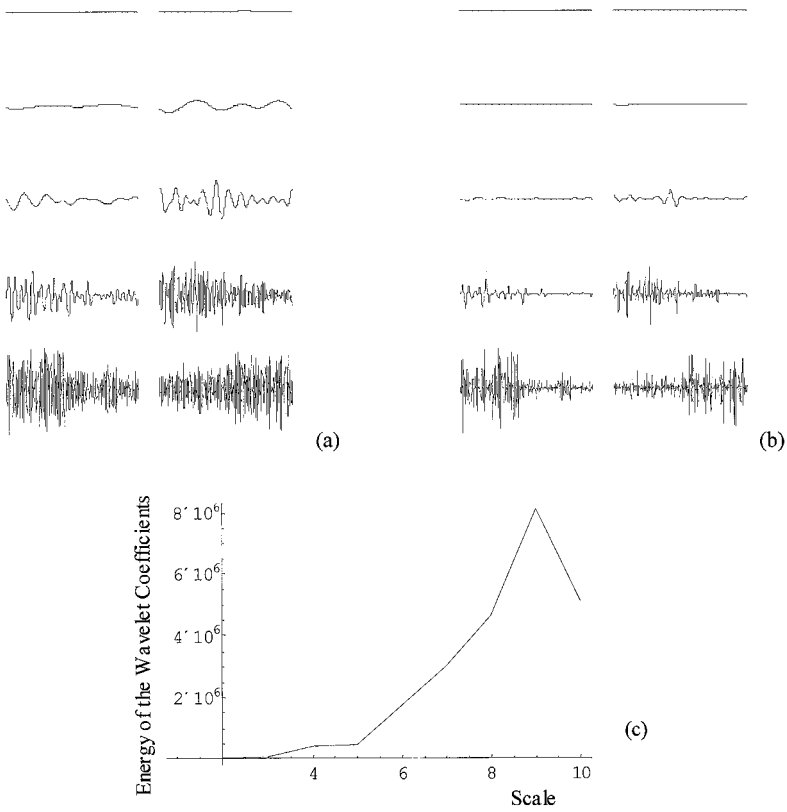

Figure 2. (a) Plot of the wavelet coefficients, value of the coefficients on the vertical axis, versus the spatial variable x, horizontal axis, at each of the 10 scales of decomposition; scale decreases from left to right and from top to bottom, i.e., scale 1 is the coarsest and scale 10 the most detailed one. Scaling of the vertical axes is the same for each plot. (b) Same as (a), but the square of the coefficients (while retaining the sign) is plotted on the vertical axes. (c) Total energy of the wavelet coefficients, vertical axis, as a function of scale (1–10), scale 10 being the finest.

The second example is a 512-point discrete signal with the same properties as the first part of the (spatially correlated) signal of Figure 1(a). Then, a nugget effect (white noise) of 20% is added to that signal. We perform the wavelet transform of these two signals and then evaluate the energy of the wavelet transform for each scale; there are nine scales since $2^9 = 512$. The plot of the wavelet coefficients at each scale is similar to that of Figure 2, for the first part. Figure 3 shows, for each scale, the percent difference between the energy of the wavelet transform of the signal with and without the nugget effect. Clearly, the nugget effect increases the energy of the wavelet transform rather dramatically for the finest scale of

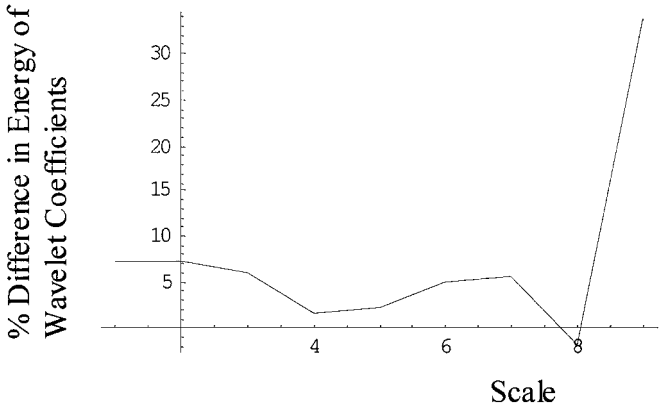

Figure 3. Percent difference between the energy of the wavelet transform of the second example signal with and without the nugget effect.

decomposition (scale 9) while the change in the other scales is rather insignificant. Thus a nugget effect influences the finest scale of decomposition of the signal by increasing the energy of the wavelet transform at that scale significantly, and this provides means for identifying a nugget effect, i.e., by examining the relative value of such energy at the finest and coarser scales of decomposition.

We perform the wavelet transform of the above example signal with the nugget effect, then set all the wavelet coefficients at the finest scale equal to zero and perform the inverse wavelet transform. This is then an application of (2) where the cutoff scale includes only the finest scale available. From the signal obtained this way, we plot the relevant variogram shown in Figure 4. Clearly, this is similar to the variogram shown in Figure 1(b), for the first part. In other words, by filtering the wavelet coefficients at the finest scale, we remove the nugget effect from the signal.

As the last example we consider the 1024-point signal plotted in Figure 5(a), which has the same statistical properties as the first part of Figure 1, yet a linear trend has been added at the first 400 points and a quadratic term for the remaining points. Figure 5(b) shows the plot of the wavelet coefficients for each scale, and Figure 5(c) shows the energy of the wavelet coefficients as a function of scale. Clearly, the trend can be seen at coarse scales, i.e., scales 2 and 3. Furthermore, the energy of the wavelet coefficients increased at scale 2 and 3, when compared to that of Figure 2(c).

DRILLING DATA AND ENTROPY ANALYSIS

The available experimental data set is from a Tunnel Boring Machine of large diameter (7.23 m) used to build a pipeline in Morocco. The object of this practical

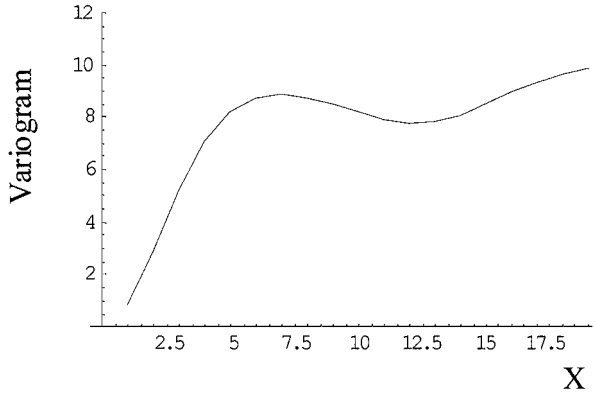

Figure 4. Variogram of the signal with nugget effect after its wavelet transform, filtering of (setting equal to zero) the wavelet coefficients at the finest scale and performing the inverse wavelet transform.

application was to take into account tunnel boring parameters to identify and quantify spatially homogeneous zones. Therefore, it is assumed that the homogeneity is achieved if the drilling data exhibits a spatially correlated stationary random process. The underlying idea is that the more the drilling variable shows a structure

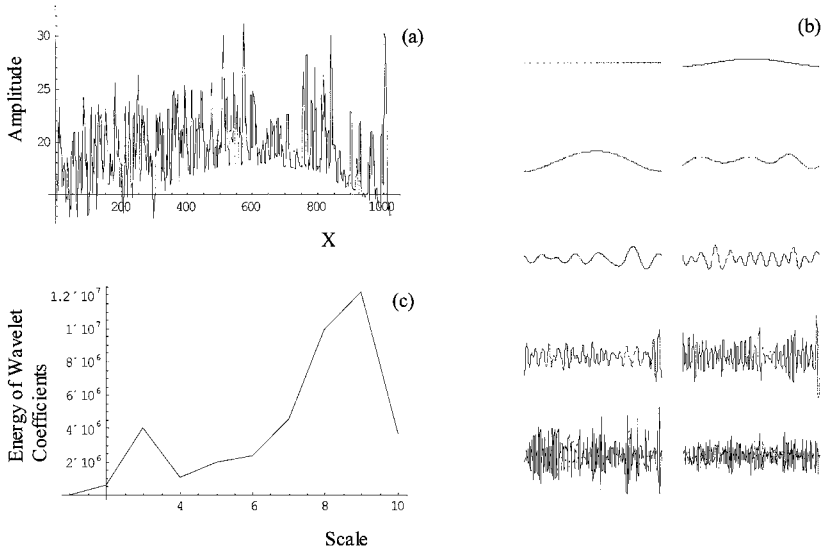

Figure 5. (a) Signal with spatially correlated structure and a trend. (b) Plot of the wavelet coefficients for each scale; scale decreases from left to right and from top to bottom, i.e., scale 1 corresponds to the coarsest scale and scale 10 to the most detailed one. (c) Energy of the wavelet coefficients for each of the 10 scales.

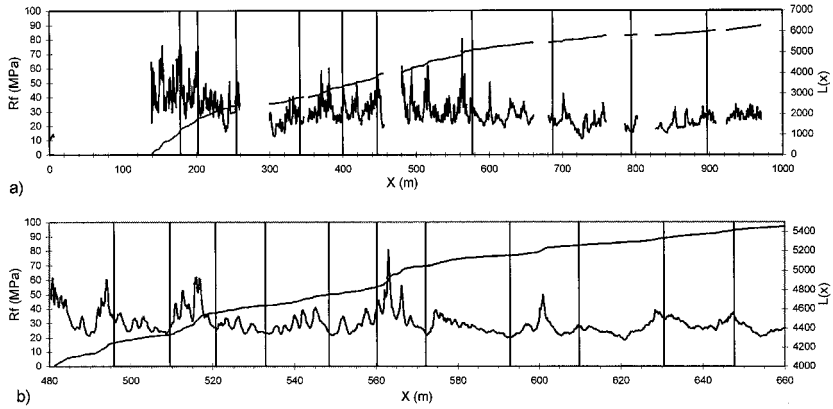

Figure 6. (a) Drilling-ability signal (*Rf*) over 1000 m studied, L function and segmenting results. (b) Drilling-ability signal (*Rf*) from 480 to 660 m, L function and segmenting results.

the fewer problems would occur because it is easier to drill a geotechnical homogeneous medium than a heterogeneous one. Thus, knowledge on expected drilling difficulties would be gained.

Several parameters were recording during drilling and three of those are used herein, i.e., thrust, penetration rate, and rotary speed. Using these three parameters in conjunction with a relevant theory (Detournay and Defourny, 1992; Gnirk and Cheatman, 1968) the so-called drilling-strength or drilling-ability can be obtained. The drilling-ability, *Rf*, depends on the type and shape of the disk cutters and can be evaluate from analytical expressions (Denis and Cremoux, 2002a). Typically *Rf* is expressed in MPa.

Figure 6 shows the drilling-ability data. Two major geological variations appear over the studied 1000 m. The first part (50–570 m) is described as a zone of tight sandstone and arkosic sandstone with some intercalation of quartzy sandstone. The second part (570–1000 m) shows pelite of lower compressive strength with some hardened schist beds. Figure 6(b) shows the plot of the *Rf* variable between 480 and 660 m. Clearly, the interface between sandstone and pelite is at about 570 m.

The concept of entropy used in this paper is based on the thermodynamics of plane curves (Dupain, Kamae, and Mendès France, 1986; Mendès France, 1983; Moore and Van Der Potten, 1989), used for analysis of signals, in Denis and Cremoux (1998, 1999, 2002b). Within the thermodynamics formalism, the entropy of a plane curve is defined in terms of the number of intersection points with a random line. The entropy of a signal is expressed as

$$H(x) = \frac{d(L(x))}{dx} \tag{4}$$

where $L(x)$ is the length of the signal (along its tortuous path) as a function of the spatial variable x, expressed as

$$L(x) = \int_0^x |X'(u)|\, du \tag{5}$$

where a prime denotes derivative with respect to the argument, and

$$\langle L(x) \rangle = \int_0^x L[|X'(u)|]\, du = \int_0^x m_{|X'|}\, du = x\, m_{|X'|} \tag{6}$$

where $m_{|X'|}$ denotes the mean of the absolute value of the spatial derivative of the process X, and $\langle \cdot \rangle$ denotes mean value. Thus, $L(x)$ is linear over a region where $m_{|X'|}$ is constant.

A complete analysis of entropy is multiscale, i.e., the regions of constant entropy are identified for continuously decreasing scales, from coarse to fine. Details on this can be found in Denis and Cremoux (1999). The example signals presented above and analyzed with wavelets have also been analyzed with entropy concepts (Denis and Cremoux, 2002 b).

Figure 6 shows the drilling-ability data and results from the analysis of the entropy of the signal, performed to evaluate regions of statistical stationarity, i.e., region of constant entropy. It appears that the entropy analysis of the *Rf* variable identifies the same main lithologic units at coarse scales as those identified by the geotechnical investigation (Fig. 6(a)) and offers a better resolution at finer scales (Fig. 6(b)) than those that can be obtained from the examination of cuttings.

WAVELET ANALYSIS OF DRILLING-ABILITY DATA COMPLEMENTARY TO ENTROPY ANALYSIS

The entropy study and the wavelet analysis complement each other. In the following, we elaborate on the complementarities. Figure 7 shows part of the drilling-ability signal and its wavelet transform. Roughly speaking, the regions of black or white identified at each scale in Figure 7(b) correspond to regions of constant entropy; theoretical investigation of this point appears in a subsequent section. Importantly, as shown in Figure 7(d), a rather dominant scale can be identified, i.e., scale 6. This, then, implies that the most useful representation of the entropy would be at that scale. This reduces the need to have representation of the entropy at several scales, which may be hard to implement in practice. Note that the energy of the wavelet coefficients is rather insignificant at fine scales, especially for the finest scale, i.e., scale 10. This implies the absence of white noise (nugget effect) in the signal, i.e., there are spatial correlations on all subregions of stationarity.

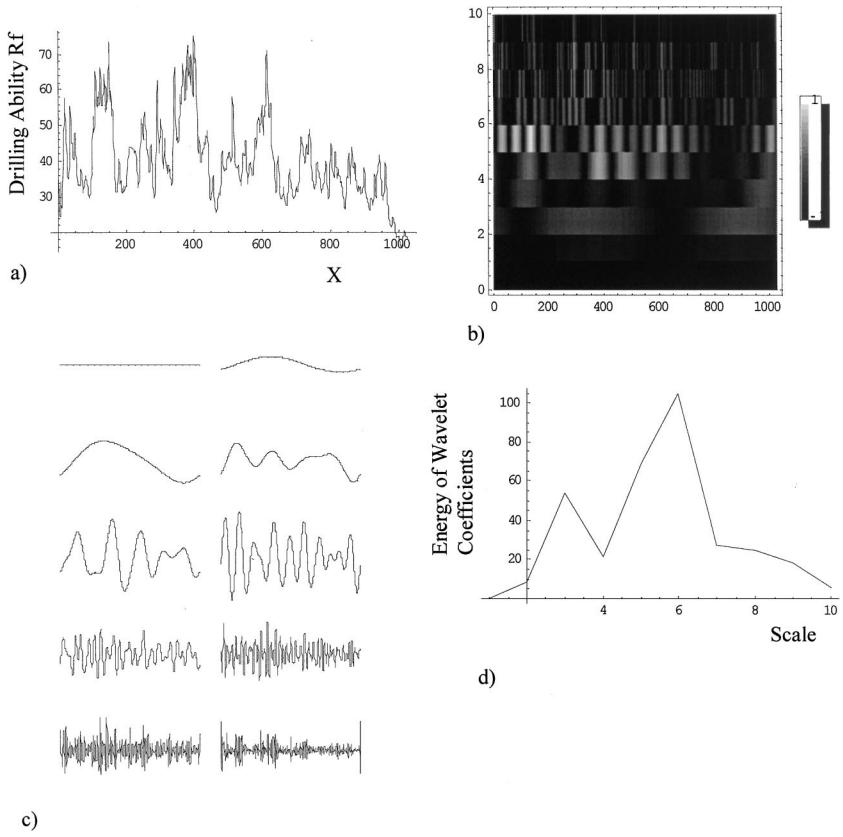

Figure 7. (a) Drilling-ability signal (*Rf*) from 138 to 240 m, i.e., 1024 discrete points. (b) Gray-scale density plot of the wavelet coefficients. (c) Plot of the wavelet coefficients for each of the 10 scales, from left to right and top to bottom; scale 1 is the coarsest and scale 10 the finest. (d) Energy of the wavelet transform (vertical axis) as a function of scale (horizontal axis).

In more detail, from Figure 7(d), it appears there are two significant scales (2 and 6). It is natural to address the geologic significance assigned to these. Scale 6 corresponds to 32 discretization spaces and scale 2 to 512 spaces. As each space is about 0.1 m, the high values of energy at scales 2 and 6 correspond to 3.2 and 51.2 m, respectively. With these values, one can obtain from entropy analysis information on "segmenting," as well as the value of entropy in each subregion. The segmenting from the coarse significant scale, i.e., scale 2 identifies the main lithologic units, i.e., those obtained from examination of the cuttings. Scale 6 offers a better resolution and makes possible to obtain a measure of homogeneity within the previously detected subregions, information which cannot be obtained by observing cuttings.

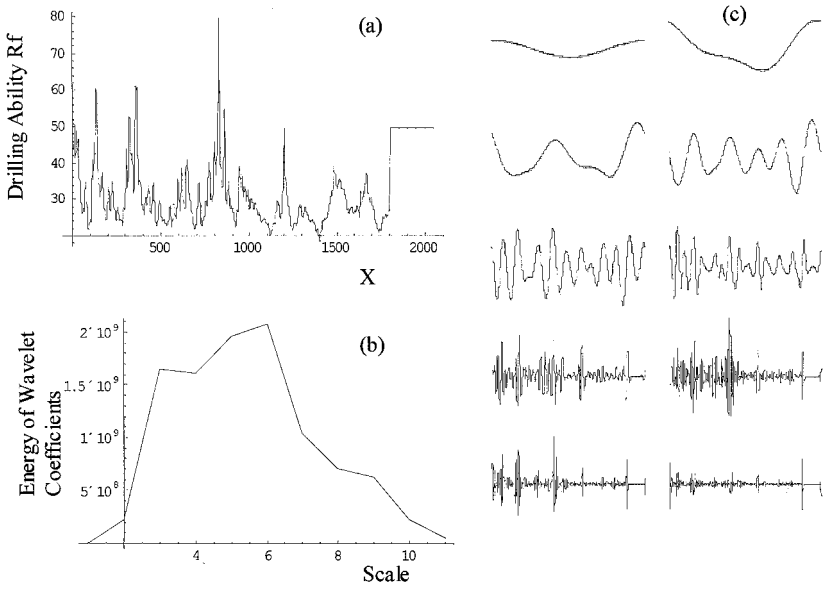

Figure 8. (a) Drilling-ability signal (*Rf*) from 480 to 660 m, i.e., 2048 discrete points. (b) Energy of the wavelet transform (vertical axis) as a function of scale (horizontal axis). (c) Plot of the wavelet coefficients for each of the 11 scales (scale 1 is not shown for simplicity), from left to right and top to bottom; scale 1 is the coarsest and scale 11 the finest.

Figure 8 is similar to Figure 7, yet for the *Rf* data from 480 to 660 m, discretized in 2048 points. There are 11 scales available for this signal. As shown in Figure 7(b), at fine scales, i.e., scales 8–11, the wavelet coefficients show overall values of higher magnitude for the part of the signal from 480 to 660 m. Note that at that depth rests the interface between a layer of sandstone and Pelites (Denis and Cremoux, 2002b). Also note the absence of nugget effect from the signal, i.e., low energy of the wavelet coefficients at fine, and especially at the finest scale 11, Figure 8(b). Furthermore, for this part of the drilling process (depth), as seen from Figure 8(b), there is not a single dominant scale, as is the case shown in Figure 7(d), but rather the range of scales from 3 to 6 is dominant. This, then, implies that a 4-scale description of the entropy would be necessary for a complete description of the regions of constant entropy.

Relation Between the Wavelet Transform and Entropy of a Function

Consider a function $f(x)$ that is random and spatially correlated in space x. The variance of the wavelet transform, $\langle [W_f(a, b)]^2 \rangle$, provides means for evaluating the energy of the wavelet transform as a function of scale a, and position b. It

can be evaluated in the Fourier space as

$$\sigma_W^2(a) = \langle [W_f(a,b)]^2 \rangle = \frac{a}{2\pi} \int_{\mathcal{R}} P_f(k) [\hat{\psi}(ak)]^2 \, dk \tag{7}$$

where $P_f(k)$ denotes the power spectrum of f and $\hat{(\cdot)}$ indicates Fourier transform. Let us first consider a process f that is stationary and spatially correlated (this corresponds to regions of stationarity of a nonstationary process). Let the autocorrelation function be of the exponential form

$$\rho(r) = \exp[-r/d] \tag{8}$$

where r denotes the separation distance between two points in x, and d denotes the correlation distance; Let the variance be σ_f^2. The Fourier transform of this autocorrelation function together with σ_f^2 provide the power spectrum of the process (Wiener–Khinchin theorem), i.e.,

$$P_f(k) = \frac{1}{\pi} \frac{\sigma_f^2 d}{1 + d^2 k^2} \tag{9}$$

Let us consider the so-called "Mexican hat" wavelet or the second derivative of the Gaussian function, and address the generality of the process in the sequence, i.e.,

$$\psi(x) = (x^2 - 1) \exp[-x^2/2] \tag{10}$$

Its Fourier transform is

$$\hat{\psi}(k) = k^2 \exp[-k] \tag{11}$$

Integral (7), for functions (9) and (11), yields

$$\begin{aligned} \sigma_W^2(a) = \langle [W_f(a,b)]^2 \rangle &= \frac{a^1}{2\pi} \int_{\mathcal{R}^1} P_f(k) [\hat{\psi}(ak)]^2 \, dk \\ &= \frac{a\sigma_f^2}{2\sqrt{\pi} d^5} (a d^2 (d^2 - 2a^2) + 2a^4 d \sqrt{\pi} \exp[a^2/d^2](1 - erf[a/d])) \end{aligned} \tag{12}$$

where $erf[\cdot]$ denotes the error function. The derivations and some of those in the sequence were performed using the program *Mathematica*. Clearly, for a fixed scale a, the energy of the wavelet transform is proportional to the variance of the

process. If a different autocorrelation function is used, e.g., of Gaussian type

$$\rho(r) = \exp[-\pi r^2/4d^2] \tag{13}$$

with variance σ_f^2 and power spectrum

$$P_f(k) = \frac{1}{\pi}\sigma_f^2 d \ \exp[-k^2 d^2/\pi], \tag{14}$$

using the wavelet expressed through (2) and (3), it follows that

$$\begin{aligned}\sigma_W^2(a) = \langle [W_f(a,b)]^2 \rangle &= \frac{a^1}{2\pi}\int_{\mathcal{R}^D} P_f(k)\,[\hat{\psi}(ak)]^2\,dk \\ &= \frac{3\pi^2\sigma_f^2}{4}\frac{a^5 d}{(\pi a^2 + d^2)^{5/2}}\end{aligned} \tag{15}$$

Again, for a fixed scale a, the energy of the wavelet transform is proportional to the variance of the process. Even though this scaling was analytically shown to hold for specific form of wavelets, straightforward numerical simulations show the generality of the process, for fixed scale a.

Now, for the cases that Rf is locally stationary with spatial correlations, the variance of the spatial derivative of the process is expressed as

$$\sigma_{Rf'}^2 = -\frac{\partial^2\left(\sigma_{Rf}^2\sigma(r)\right)}{\partial r^2} \tag{16}$$

Clearly, for locally stationary process Rf the variance of its spatial derivative Rf' is proportional to the variance of Rf, and thus $(m_{|Rf'|})^2$ is proportional to the energy of the wavelet transform for each fixed scale a. This can be seen precisely for Rf being Gaussian, where now its derivative is also Gaussian (with zero mean) and the following holds (Vanmarcke, 1983, p. 156).

$$m_{|Rf'|} = \sqrt{\frac{2}{\pi}}\sigma_{Rf'} \tag{17}$$

Finally, note that, in general,

$$\sigma_f^2 = \sigma_W^2\, g(a,d) \tag{18}$$

holds, where, for the case of (15)

$$g(a,d) \approx \frac{(\pi a^2 + d^2)^{5/2}}{a^5 d} \tag{19}$$

which is a function continuously decreasing with a. This implies that information increases towards small scales. Thus, in a sense, the dominant scale or scales identified by the wavelet analysis are the minimum scales for which information from the entropy analysis is most useful. This point is presently being investigated further and will be presented elsewhere.

CONCLUSIONS

Entropy analysis of boring data is capable of identifying subregions of stationarity, which can be treated with standard geostatistical methods. Its multiscale nature provides rich data, yet a full—at all scales, from support to domain—entropy may be overwhelming for use in drilling practice. Using wavelet analysis scales containing the most useful information can be identified, thus the wavelet analysis complements the entropy one nicely. This is demonstrated in the paper through the interaction of the wavelet with the entropy analysis. The interaction at this stage is not dynamic, since both analyses are performed independently and the wavelet analysis sort of feeds information to the entropy one. The present study is amenable to a dynamical interaction, the theoretical basis of which need to be established.

ACKNOWLEDGMENTS

The present study initiated before and advanced further during the Summer 2001 visit of GF to CDGA, Bordeaux. GF acknowledges the opportunity for the visit. Support from NSF under grant No. CMS-9812834 is gratefully acknowledged.

REFERENCES

Daubechies, I., 1992, Ten lectures on wavelets: Society for Industrial and Applied Mathematic (SIAM), Philadelphia, PA, 357 p.

Denis, A., and Cremoux, F., 1999, Structural analysis of a signal from entropy tool-application to tunnel boring data, *in* Melchers, R. E., and Steward, M. G., eds., Application of statistics and probability, ICASP 8, Sidney, 12–15 December, Vol. 1, p. 401–405.

Denis, A., and Cremoux, F., 2002a, Traitement et analyse des paramètres de pilotage d'un tunnelier: Can. Geotech. J., v. 39, p. 451–462.

Denis, A., and Cremoux, F., 2002b, Using the entropy of curves to segment a time or spatial series: Math. Geol., v. 34, no. 8, p. 899–914.

Denis, A., Cremoux, F., and Lapeyre, E., 1998, Utilisation des paramètres de pilotages d'un tunnelier pour une recherche et une quantification automatique des zones homogènes, *in* Miresco, E. T., ed., First International Conference on New Information Technologies for Decision Making in Civil Engineering, Montreal, 11–13 October, Vol. 1, p. 733–744.

Detournay, E., and Defourny, D., 1992, A phenomenological model for the drilling action of drags bits: Int. J. Rock Mech. Min. Sci., v. 29, p. 13–23.

Dupain, Y., Kamae, T., and Mendès France, M., 1986, Can one measure the temperature of a curve: Arch. Ration. Mech. Anal., v. 94, p. 155–163.

Frantziskonis, G., and Deymier, P. A., 2000, Wavelet methods for analyzing and bridging simulations at complementary scales—The compound wavelet matrix and application to microstructure evolution: Model. Simul. Mater. Sci. Eng., v. 8, p. 649–664.

Frantziskonis, G., and Hansen, A., 2000, Wavelet-based multiscaling in self-affine random media: Fractals, v. 8, p. 403–411.

Frantziskonis, G., Simon, L. B., Woo, J., and Matikas, T. E., 2000, Multiscale characterization of pitting corrosion and application to an aluminum alloy: Eur. J. Mech., v. 19, p. 309–318.

Gnirk, P. F., and Cheatman, J. R., 1968, A theoretical description of rotary drilling for idealized down hole bit rock conditions: Soc. Pet. Eng. J., v. 246, p. 443–450.

Mendès France, M., 1983, Les courbes chaotiques: Courrier C.N.R.S., v. 51, p. 5–9.

Moore, R., and Van Der Potten, A., 1989, On the thermodynamics of curves and other curlicues, *in* Proceedings of Conference on Geometry and Physics, Canberra, p. 82–109.

Vanmarcke, E., 1983, Random fields: MIT Press, Cambridge, MA, 382 p.